Fabrication and Characterisation of Miniature Parabolic Acoustic Lenses

Erwin J Alles*, Daniil Nikitichev* and Adrien E Desjardins
Department of Medical Physics & Biomedical Engineering,
University College London, London, United Kingdom.
Email: E.Alles@UCL.ac.uk

***Abstract*—As recently demonstrated, all-optical B-mode ultrasound imaging can be performed with a pair of coated optical fibres for transmission and reception that is translated to create a virtual array of elements. However, with translation in the in-plane dimension, the small lateral dimensions of the fibres results in out-of-plane acoustic divergence, which leads to image clutter and loss of sensitivity.**

This study is focussed on the fabrication of acylindrical acoustic lenses to provide an acoustic focus in the out-of-plane dimension. Two fabrication methods were considered: laser-cutting of acrylic (PMMA), and 3D-printing of VeroWhite Plus (VWP). Using acoustic transmission measurements, the acoustic properties of PMMA (speed of sound: 2750 **m/s, differential attenuation coefficient:** 0.5 **dB/cm/MHz at** 5 **MHz) and VWP (**2539 **m/s,** 4.0 **dB/cm/MHz at** 5 **MHz) were determined and subsequently used to optimise the lens shapes for both materials by means of a genetic algorithm.**

With both methods, lenses that accurately reproduced the designed shape were manufactured. However, the out-of-plane focus achieved with the 3D-printed VWP lens was closer to the modelled field focus than that generated by the laser-cut PMMA lens. In addition, while the acoustic attenuation coefficient of the former was eight times greater than that of the latter, the acoustic field propagated through both lenses had very similar fractional bandwidths of around 160%**, centered around** 15 **MHz. This study highlights the potential benefits of 3D-printed VWP lenses over laser-cut PMMA lenses for diagnostic ultrasound applications.**

I. Introduction

Fibre-optic pulse-echo ultrasound sensors can provide high bandwidths and sensitivity that make them attractive for B-mode ultrasound imaging, particularly for minimally invasive applications. Recently, 2D B-mode imaging of soft tissue structures was performed by translating a pair of optical fibres for transmission and reception in the in-plane dimension, thereby creating a virtual array of transducer elements [1]. Due to the small lateral dimensions of the optical fibres, there is pronounced acoustic divergence in the out-of-plane dimension, which leads to clutter and loss of sensitivity.

To overcome this limitation, acoustic lenses can be used to focus the acoustic field in the out-of-plane dimension. This approach is typically used in conventional 2D clinical imaging probes that are positioned on the patient skin [2]. Such acoustic lenses are typically fabricated using a casting-based method [3], and developing the required mold can be costly and time-consuming. In addition, for best results, collimating acoustic lenses should have non-circular surfaces [3], which can be challenging with some manufacturing methods.

This study involved a comparison of two methods for acoustic lens creation: laser-cutting and 3D-printing. The former is suitable for acylindrical lenses (defined as having non-circular curvature in one dimension only) that are cut from a planar sheet; the latter can generate lenses with arbitrary shapes. Both methods are suitable for rapid, low-cost fabrication. Whilst the accuracy of these methods is highly dependent on the systems and parameters used, the high accuracies achieved recently (tens of μm [4, 5]) are attractive for ultrasonic lenses. For computational expediency, we limited our acoustic lens shapes to two concave parabolic surfaces. Using a fibre-optic transmitter as a source, field measurements of the acoustic fields transmitted through these lenses were performed and their frequency contents were analysed.

II. Methods

The acoustic lenses tested in this work were either cut from 6 mm thick sheets of cast acrylic (PMMA) using a laser cutter (50 W VLS4.60, Universal Laser Systems, Scottsdale, AZ), or printed in VeroWhite Plus (VWP) using a 3D-printer (Objet 30 Pro, Stratasys, Israel). To measure the acoustic properties of PMMA and VWP, differential acoustical transmission measurements were performed in water with a pulser/receiver (5077PR, Olympus Panametrics, Waltham, MA) and two planar ultrasound transducers spaced 50 mm apart (5 MHz centre frequency, V310, Olympus Panametrics, Waltham, MA). For these measurements, 6 mm thick planar samples were used. The speed of sound was computed from time-of-flight differences between measurements performed with and without each sample, and the time-of-flight was determined using the Akaike information criterion [6]. The differential acoustical attenuation coefficient at 5 MHz was determined from the slope of the linear fit to the difference between the log-transformed power spectra obtained with and without each sample.

Parabolic acylindrical lens shapes were defined by the set of parameters indicated in Fig. 1. For structural integrity and ease of handling, all considered lens shapes had a height $h = 10$ mm, a narrowest thickness $n = 0.5$ mm, and a focal

*These authors contributed equally to this work, which was funded through the European Research Council Starting Grant 310970 MOPHIM.

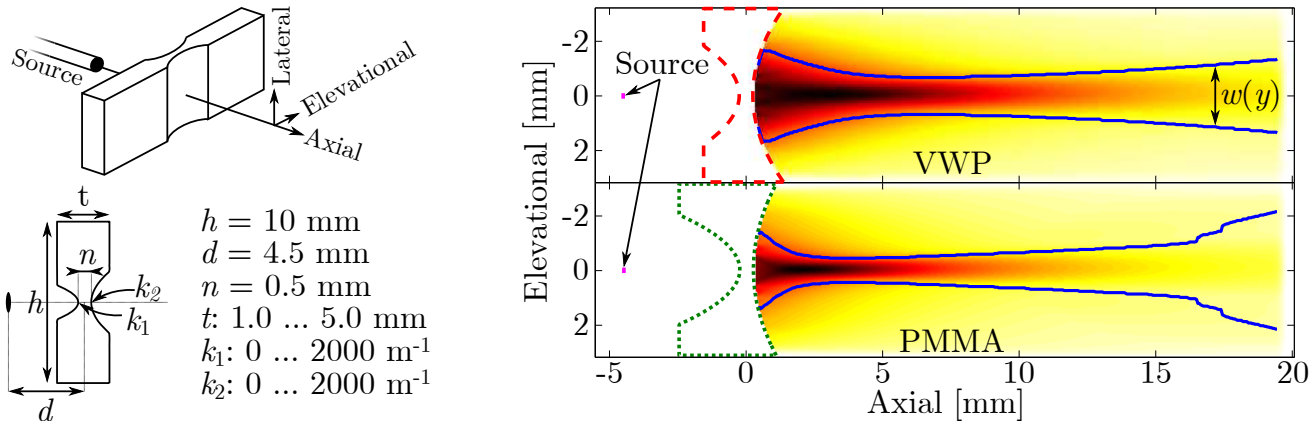

Fig. 1. **Left:** sketch of the lens geometry, source location, and shape parameters and their ranges. **Right:** Maximum amplitude projections of the simulated pressure field generated by the optimal design for a 3D-printed lens (VeroWhite Plus, top) and a laser-cut lens (PMMA, bottom). The blue curves indicate the elevational width of the full-width, half-maximum beam waist as a function of axial depth.

distance $d = 4.5$ mm. There were three free parameters: the thickness t, and the on-axis curvatures of the lens surfaces k_1 and k_2. A two-dimensional acoustic k-Wave model [7] was used to propagate the acoustic field generated by a 200 µm long line source through the lenses defined by each set of parameters. The spatial grid consisted of 128×512 points spaced 50 µm apart, and a fluid model was used for simplicity as it yielded acoustic fields very similar to those computed using the elastic formulation (data not shown). The measured values for the speed of sound and attenuation coefficient in water, VWP and PMMA were used in these calculations.

The free parameters were optimised using a custom genetic algorithm [8] implemented in MATLAB to obtain an acoustic field that was collimated in the plane of the lens. The fitness F_i of each set of parameters i was determined as

$$F_i = Q_{\text{amp}} \cdot Q_{\text{shape}}^2. \tag{1}$$

Here, the amplitude factor Q_{amp} is computed as the normalised mean over axial depths y of the maximum pressure p observed in elevational distance x and time t, i.e.,

$$Q_{\text{amp}} = \underset{y}{\text{mean}} \left[\max_{x,t} p(x,y,t) \right] / \max_{x,y,t} p(x,y,t), \tag{2}$$

and the shape factor Q_{shape} as the normalised mean of the waist width w,

$$Q_{\text{shape}} = \underset{y}{\text{mean}} \left[w(y) \right] / \max_{y} w(y), \tag{3}$$

where $w(y)$ is the elevational width at depth y where $\max_t p(x,y,t) \geq \frac{1}{2} \max_{x,t} p(x,y,t)$. For the best lenses found for both 3D-printed VWP and laser-cut PMMA, the boundaries of this elevational region are displayed, superimposed on a maximum amplitude projection ($\max_t p(x,y,t)$) of the pressure field, in Fig. 1.

In the custom genetic algorithm, a population size of 100 was evolved for 50 generations, where the best 15 members of each generation evolved unchanged, the worst 7 members were completely randomised in every generation, the likelihood for members to be picked for procreation was proportional to the e-base exponent of the member's fitness ranking, the parameters t, k_1 and k_2 were allowed to mutate randomly by at most 10 % of the parameter range, and parameter crossover was entirely randomised.

To create the acoustical source, an optical fibre with a core diameter of 200 µm was dip-coated with a 25 µm thick composite of PDMS and carbon nanotubes using the process described in [9]. Illumination of the coating through the fibre core was performed with pulsed laser light (2 ns pulse duration, 1064 nm, 35 µJ pulse energy, SPOT-10-500-1064, Elforlight, UK), and through the photoacoustic effect a broad-band acoustic field was transmitted. This field propagated through the acoustic lens and was subsequently detected optically using a custom planar Fabry-Pérot etalon with a thickness of 10 µm exhibiting a broadband sensitivity of $0 - 110$ MHz [10]. Using a custom 3D-printed holder, the source fibre was centered with respect to the acoustic lens, with its distal end located at a distance of 4.5 mm from the acoustic lens; the etalon was located on the other side of the lens at a distance of 7 mm from the lens centre with its surface perpendicular to the axial direction. Measurements in the absence of a lens were performed with the same distance between the source fibre and etalon (11.5 mm).

The measured acoustic fields were propagated backwards and forwards in time using the angular spectrum approach [11]. At different time points, the spatial location corresponding to the maximum acoustic amplitude was determined, along with the -3 dB area around this location where the acoustic amplitude was greater than half the maximum amplitude defined the beam waist. To evaluate the acoustic collimation (or divergence in the absence of a lens), the spatial extent of the beam waist at each distance was measured in the lateral and elevational directions.

III. Results

Acoustic transmission measurements of cast acrylic (PMMA) yielded a sound speed of 2750 m/s and a differential attenua-

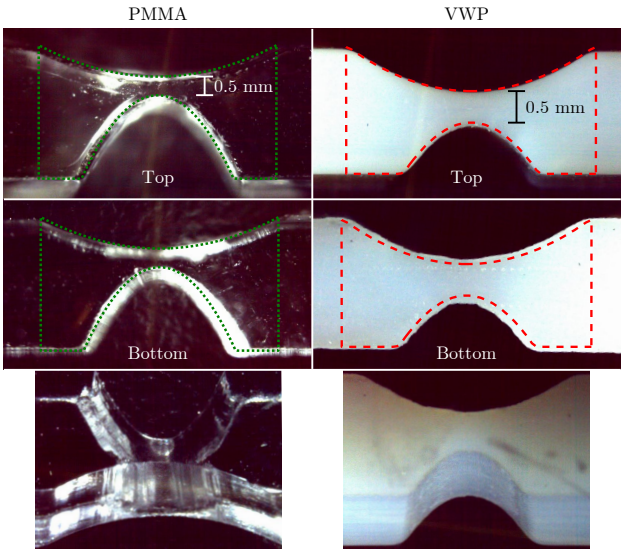

Fig. 2. **Left:** microscope images of the laser-cut lens. The designed shape is indicated in dotted lines. The laser-cutting light was incident from the top. The bottom panel contains a perspective view of the same lens. **Right:** Microscope images of the 3D-printed lens, together with the designed shape (dashed line). The bottom panel shows a perspective view.

tion coefficient of 0.5 dB/cm/MHz at a frequency of 5 MHz. For 3D-printed VeroWhite Plus (VWP), values of 2539 m/s and 4.0 dB/cm/MHz were found. The density of both PMMA and VWP was approximately 1180 kg/m^3.

The acoustic lenses fabricated with laser-cutting and 3D-printing had shapes that closely followed the optimised designs (Fig. 2). However, variations in the shape along the lateral dimension were apparent, leading to slight differences in the shape of the top- and bottom profiles. Additionally, both lenses exhibited surface roughness on the order of ≤ 20 µm. Laser cutting appeared to introduce small bubbles with diameters of several tens of µm into the PMMA which were not present in the raw material. The perspective view of the 3D-printed lens revealed the layered structure inherent to the printing process, but due to the opacity of VWP no information could be gained on the internal structure.

The pressure field measurements (Fig. 3, left) revealed that the acoustic energy was more confined in the elevational direction with both lenses. In the case of the 3D-printed lens, the elevational extent of the -3 dB half-amplitude contours (black lines, left panel) was virtually independent of the axial distance (right panel, ranging between $0.53 - 1.03$ mm for distances between $1 - 13$ mm), which indicates that the acoustic energy was effectively collimated. With the laser-cut lens, less effective collimation was achieved: a sharper focus was observed at an axial distance of 1 mm, and the elevational beam width ranged between $0.35 - 3.3$ mm.

In the absence of a lens, the acoustic pulse recorded at a distance of 7 mm exhibited a fractional acoustic bandwidth of 109% (-6 dB) around a centre frequency of 25 MHz (Fig. 4). In the presence of either lens, the fractional bandwidth increased to 160% while the centre frequency decreased to 15 MHz. Based on the measured differential attenuation coefficient, this reduction in absolute bandwidth was expected for a VWP lens. However, for a PMMA lens, which was fabricated with material that was less attenuating prior to cutting, a wider bandwidth was expected. This observation suggest that material imperfections introduced during manufacturing (such as surface roughness, bubble formation or material inhomogeneities) resulted in additional attenuation within the PMMA lens.

IV. Discussion and Conclusion

The results presented in this work demonstrate that acylindrical lenses laser-cut from cast acrylic (PMMA) or 3D-printed in VeroWhite Plus (VWP) both effectively focussed the acoustical energy in the elevational direction. In the case of the VWP lens, excellent collimation was achieved in both simulations and experiments, which confirms that the algorithms used to design the lenses were both reasonably accurate and able to find good lens shapes, despite being stochastic in nature.

While good collimation was achieved in this work, employing these lenses in an imaging setting requires further research. The acoustic inhomogeneities introduced by adding a lens need to be taken into account during image reconstruction. However, this requires knowledge of the lens shape at greater accuracy than currently available, and suitable algorithms are numerically expensive.

Both lenses fabricated from VWP and PMMA exhibit significant acoustical attenuation. In the former case the attenuation is inherent to the material; in the latter case, the attenuation is likely introduced during fabrication. The attenuation within an acrylic lens could potentially be reduced by 3D printing rather than laser cutting the lens, as this could yield lenses that are optically clear and smooth [12] (and hence free from micro-bubbles). In addition, 3D printing allows for arbitrary, three-dimensional lens shapes, whereas laser cutting can yield only (a)cylindrical lenses.

In conclusion, we have demonstrated that, using laser cutting and 3D printing, acylindrical acoustic lenses can be fabricated that effectively focus the acoustic energy while maintaining a high bandwidth. With appropriate imaging algorithms, acylindrical acoustic lenses are hence expected to result in significant clutter reduction in 2D B-mode images obtained using, e.g., fibre-based acoustic sources and detectors. Additionally, with 3D-printing, there is the potential to manufacture acoustic lenses with curvature in two directions, allowing for a wider range of applications such as high-intensity focussed ultrasound, acoustical microscopy, or acoustic tweezers.

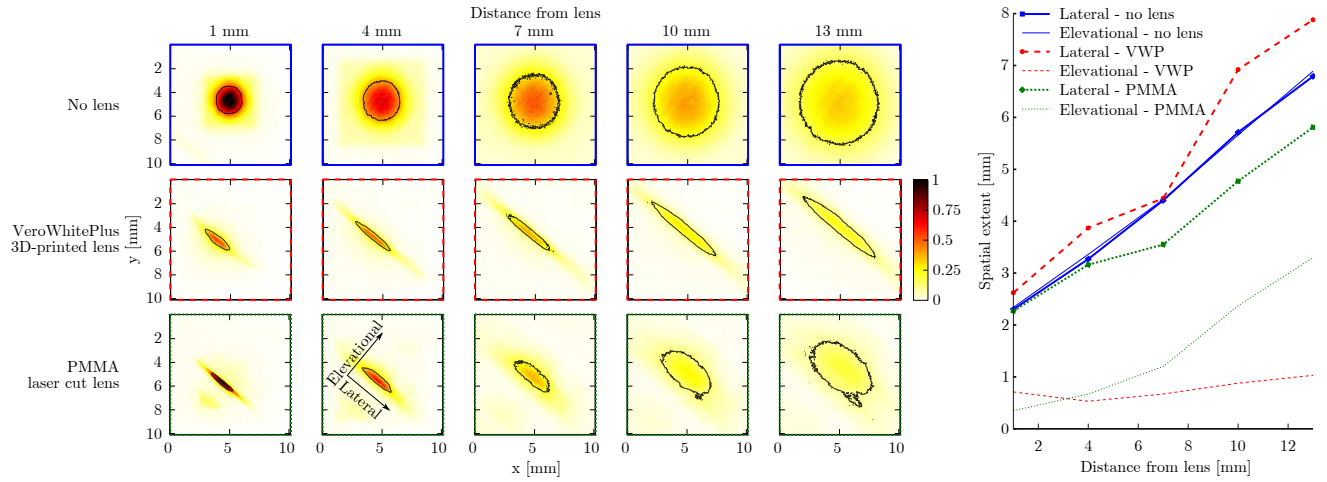

Fig. 3. **Left:** maximum amplitude of transient pressure fields observed at several distances from the lens. Pressure fields were measured at a distance of 7 mm, and numerically propagated to the remaining distances. Black contours indicate where the pressure amplitude dropped below half of the maximum amplitude at each distance. Top: no lens, middle: 3D-printed VWP lens, bottom: laser-cut PMMA lens. Amplitudes are displayed (on a linear scale) in Volts, as the acoustic detector was not calibrated. **Right:** the spatial extents of the half-amplitude contours in the lateral (thick lines) and elevational (thin lines) directions are measures of the acoustical beam profile as a function of distance. Data acquired without a lens (measured at the position coinciding to a distance of 7 mm beyond the PMMA lens) is shown using solid lines; data from the 3D-printed VWP and laser-cut PMMA lenses are shown using dashed and dotted lines, respectively.

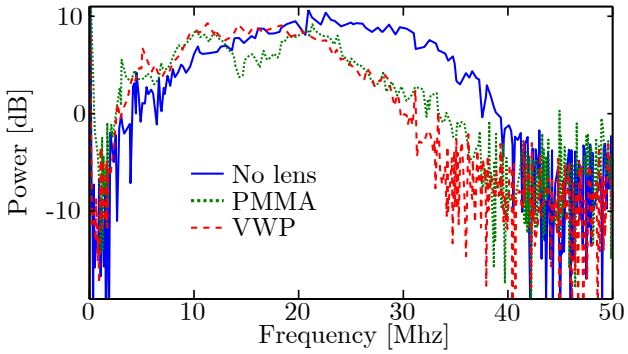

Fig. 4. Power spectra of the A-scans corresponding to maximum acoustic amplitude, obtained using no lens (solid blue line), a laser-cut PMMA lens (dotted green line), or a 3D-printed VWP lens (dashed red line).

References

[1] RJ Colchester, EZ Zhang, CA Mosse, PC Beard, I Papakonstantinou, and AE Desjardins. Broadband miniature optical ultrasound probe for high resolution vascular tissue imaging. *Biomedical Optics Express*, 6(4):1502–1511, 2015.

[2] Y Yamashita, Y Hosono, and K Itsumi. Effects of metal particle dopant on acoustic attenuation properties of silicone rubber lens for medical echo array probe. *Japanese journal of applied physics*, 44(6S):4558, 2005.

[3] KT Corbett, F Middleton, and R Sternberg. Nonspherical acoustic lens study. *The Journal of the Acoustical Society of America*, 59(5):1104–1109, 1976.

[4] Neona. VLS4.60 Specifications, http://neona.com/en/product/491/cat/285, 2015.

[5] Stratasys. Objet30 Pro Specifications, http://www.stratasys.com/3d-printers/design-series/objet30-pro, 2015.

[6] C Li, L Huang, N Duric, H Zhang, and C Rowe. An improved automatic time-of-flight picker for medical ultrasound tomography. *Ultrasonics*, 49(1):61–72, 2009.

[7] BE Treeby and BT Cox. k-wave: Matlab toolbox for the simulation and reconstruction of photoacoustic wave fields. *Journal of biomedical optics*, 15(2):021314–021314–12, 2010.

[8] M Mitchell. *An introduction to genetic algorithms*. MIT press, 1998.

[9] RJ Colchester, CA Mosse, DS Bhachu, JC Bear, CJ Carmalt, IP Parkin, BE Treeby, I Papakonstantinou, and AE Desjardins. Laser-generated ultrasound with optical fibres using functionalised carbon nanotube composite coatings. *Applied Physics Letters*, 104(17):173502, 2014.

[10] E Zhang, J Laufer, and P Beard. Backward-mode multiwavelength photoacoustic scanner using a planar fabry-perot polymer film ultrasound sensor for high-resolution three-dimensional imaging of biological tissues. *Applied optics*, 47(4):561–577, 2008.

[11] X Zeng and RJ McGough. Optimal simulations of ultrasonic fields produced by large thermal therapy arrays using the angular spectrum approach. *The Journal of the Acoustical Society of America*, 125(5):2967–2977, 2009.

[12] LuxExcel. LuxExcel Printed Optics, https://www.luxexcel.com/printed-optics/, 2015.